J Mater Sci (2011) 46:3935–3941
DOI 10.1007/s10853-011-5318-x

Tensile properties of fly ash/polyurea composites

Jing Qiao · Gaohui Wu

Received: 25 October 2010 / Accepted: 22 January 2011 / Published online: 5 February 2011

Abstract In this article, composites with polyurea as the matrix were prepared. Fly ash (FA) is a waste product of thermal power stations generated in huge quantities and consists of hollow particles with porous shells. These particles were employed as the filler. The volume fraction and particle size of FA were varied to study their effects on the density and tensile properties of the composites. The tensile tests were performed using an Instron load frame combined with a digital camera. Scanning electron microscopy (SEM) was used to observe the fracture surfaces of the composites. Results indicated that the addition of FA linearly decreased the density of the composites. Tensile stress and elongation at break of all composites decreased with an increasing volume fraction of FA. The moduli at 100 and 300% elongation of the composites with small- or medium-sized FA particles increased up to a certain value and declined with further addition of FA. Fractographic analysis showed that large FA particles were crushed, while finer particles tended to debond.

Introduction

Polyurea (PU) is a product from the chemical reaction between an isocyanate and an amine [1]. It is a stable and 100% solid polymer system that is insensitive to humidity and low temperatures. Furthermore, it exhibits excellent properties including high thermal stability, abrasion and corrosion resistance, and superior mechanical properties. These can be controlled over a broad range from soft rubber to hard plastic by varying the chemistry [2, 3]. Some PUs are able to reach tensile strengths of 6000 psi and strains of over 500% [4]. In virtue of these advantages, it becomes an outstanding candidate for a coating system that can be applied to a myriad of applications including concrete coating, truck-bed liners, marine coatings, railcar linings, etc. [5]. Recently, it has been used either as a protective coating on metallic structures or as a layer between the outer facesheet and the foam core in a blast-tolerant sandwich structure [1]. These attributes can be greatly enhanced by optimal microstructural modifications, e.g., the addition of fillers. In order to avoid increasing the overall density, the hollow particle with low density becomes an excellent option.

Fly ash (FA), which consists of hollow particles with porous shells, is a waste residue generated during coal combustion for energy production. It makes up a major proportion of industrial by-products; however, less than 35% is recycled. Dumped FA occupies valuable land and poses a potential environmental hazard from the leaching of metals. Hence, the recycling of FA has become an increasing concern in recent years. Many attempts have been made to utilize FA meaningfully in the chemical field [6, 7], agricultural field [8], and cement and construction industries [9, 10]. It has also been used as a filler in composites with metal [11–14] or polymer [15–23]. As the main components of FA are inorganic, incorporation of FA particles can increase the hardness and stiffness of the composites, while decreasing the strength. Chand [15] studied the effect of FA on the mechanical properties of unsaturated polyester composites and found that increasing the volume fraction of FA reduces the tensile and impact strengths of the composites. This agrees with the study by Kishore et al. [16] and Srivastava et al. [17] for an epoxy composite system. However, Chalivendra and Shukla [18] showed that the addition of FA particles increases the specific tensile strength of FA filled polyurethane composites for all

J. Qiao (✉) · G. Wu
School of Materials Science and Engineering,
Harbin Institute of Technology, Harbin 150001, China
e-mail: jingqiao.hit@gmail.com

volume fractions due to the decrease in density after the addition of cenospheres. Its porous structure may improve some special properties of the composites, for example, the electromagnetic interference shielding, damping properties, and energy absorption. Wu et al. [13] studied the damping properties of aluminum–fly ash composites. They found that the damping capacity of the 6061 Al alloy has been improved by the addition of FA particles, especially when measured using a bending-vibration mode. The damping capacity of the FA/6061 Al composites was more than four times that of the 6061 Al. Gu et al. [20, 21] evaluated the effect of porosity and volume fraction of FA on the damping properties of modified epoxy composites filled with FA. The results suggested that the tanδ values of the composites filled with 30–50 vol% FA are nearly twice that of the matrix in the frequency range of 100–800 Hz. Dou et al. [14] conducted a high strain rate compression test on cenosphere-pure aluminum syntactic foams, showing a $\sim$45–60% increase in dynamic compressive strength and a $\sim$50–70% increase in energy absorption capacity compared with quasi-static compression.

Based on the above discussion, FA was selected as the filler to make composites with PU as the matrix. PU filled with FA (FA/PU) composites could potentially be used as a protective coating or as a layer in a blast-tolerant sandwich structure, with lower overall density and material cost. In our previous study [24], FA/PU composites were prepared for the first time, and their dynamic mechanical properties over the temperature range from -80 °C to 70 °C were studied. The results revealed that both the storage and loss moduli increase significantly with loading of FA particles. When the volume fraction of FA increases to 30%, the storage and loss moduli of FA/PU composites are more than 2.5 times those of the unfilled PU at room temperature. However, the quasi-static mechanical properties of FA/PU composites are not reported in the literature, which are useful to understand the microstructure of the composites, e.g., the interfacial bonding condition and are basic polymer properties for the engineering application of this kind of composites. Moreover, no published study on the quasi-static mechanical properties of composites with PU as the matrix exists. In this study, quasi-static tensile tests were performed, and the effects of volume fraction and particle size of FA on the mechanical properties of the composites, e.g., tensile stress at break, elongation at break, moduli at 100 and 300% elongation, are identified.

Experimental

Material

Composites were fabricated using PU as the matrix and FA as inclusions. PU elastomer was prepared by the reaction of poly(tetramethylene oxide-di-*p*-aminobenzoate) (Versalink P-1000; Air Products) with a polycarbodiimide-modified diphenylmethane diisocyanate (Isonate 143L; Dow Chemical). The chemical structures of these two components are shown in Fig. 1. FA was supplied by the Harbin Thermal Power Station in China. It was sieved with a standard mesh sieve column on a mechanical shaker, and the particle sizes in the range of <75, 105–149 μm, and 177–420 μm in diameter were used in this study. Properties of the FA particles are tabulated in Table 1.

Preparation of composites

FA particles, which were preheated at 110 °C for 1 h and stored in a desiccator for use, were introduced into Versalink P-1000 in a predetermined proportion. Using a magnetic stirrer, the mixture was stirred for 2 h while being degassed to achieve a homogenous distribution. Meanwhile, the Isonate 143L was degassed separately until most of the entrapped air bubbles were removed. These two components were then mixed rapidly for 5 min while degassing. Finally, the mixture was cured in a PDMS (polydimethylsiloxane) mold at room temperature for 1 week. In order to control humidity levels, the mold was placed in an environmental chamber that maintained a relative humidity level of 10%. As stated previously, FA particles in three size regions were

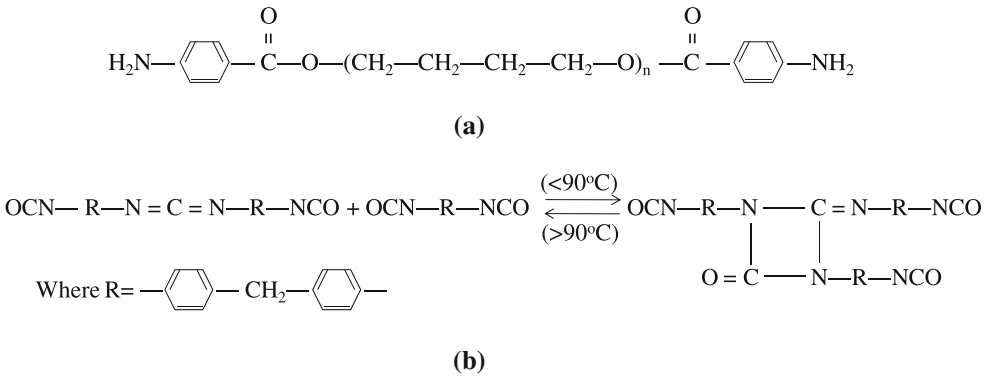

Fig. 1 Structures of Versalink P1000 (**a**) and Isonate 143L (**b**)

Table 1 Properties of FA particles

Size (μm)	Density (g/cm^3)	Porosity (%)	Relative wall thickness (t/R)
<75	0.714	68.2	0.120
105–149	0.781	64.3	0.137
177–420	0.977	55.7	0.177

t wall thickness; R radius of FA particle

employed. For each size, volume fractions of the particles in the final composite were 5, 10, and 20%, respectively. Consequently, a total of ten material configurations were prepared, including pure PU.

Tests

Density characterization

The density of the composites (ρ) was determined by Archimedes' drainage method. The density of the specimen was measured in both air and water. ρ was calculated from the relation:

$$\rho = \frac{m_{\text{Air}}}{m_{\text{Air}} - m_{\text{Water}}} \cdot \rho_{\text{Water}} \quad (1)$$

where m_{Air} and m_{Water} are the mass of the composites in air and in water, respectively, and ρ_{Water} is the density of water. For each material configuration, five specimens were measured, and an average value was reported.

Measurement of mechanical properties

Mechanical properties such as tensile stress at break, elongation at break, moduli at 100 and 300% elongations were determined by subjecting dumbbell-shaped specimens (according to the ASTM standard testing procedure D 412 for elastomers) to an Instron load frame with a 1 kN Interface model 1500ASK-200 load cell. The gage length of the specimen was 25 mm. The speed of the crosshead was 76.2 mm/min. A digital camera was used to take a picture of the specimen every 10 s during testing. By analyzing these pictures, the strain of the specimen was obtained. Thereby, the tensile stress–strain curves were determined. Three specimens of each material configuration were tested, and average values were reported.

Scanning electron microscopy

Fractured surfaces of the composite specimens from tensile testing were examined with a Philips XL30 ESEM scanning electron microscope (SEM) at an accelerating voltage of 5 kV. Due to poor conductivity, the specimens were coated with a thin layer of iridium (75-nm thick) in an automatic sputter coater.

Results and discussion

Density characterization

Densities of the FA/PU composites were determined for all volume fractions and particle sizes of FA. Figure 2 shows the variation of density as a function of FA content. It is interesting to observe that the density of the composites relies more on FA content rather than on FA particle size. Owing to the lower density of FA particles (given in Table 1) compared with unfilled PU (1.10 g/cm^3), the density of the composites decreases linearly with increasing FA content. For example, with a FA volume fraction of 20%, the density of the composites decreases more than 8% compared with that of the unfilled PU. The lower density of the composites filled with larger FA particles at high volume fraction may be caused by air bubbles introduced during the fabrication procedure.

Mechanical properties

Stress–strain curves

Figure 3 shows typical engineering stress–strain curves of the unfilled PU and FA/PU composites for different volume fractions. The unfilled PU and FA/PU composites both show typical elastomeric tensile behavior. As shown in Fig. 3, almost all the stress–strain curves can be divided into three regions: an initial linear elastic region, a plateau region, and a terminal nonlinear increasing region before

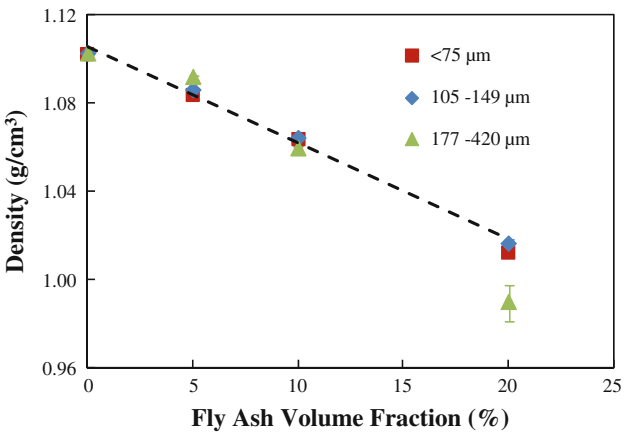

Fig. 2 The density of FA/PU composites as a function of volume fraction of FA (the error bars represent the standard deviation, the central points are the average values of five results, and the *dashed line* is the trendline)

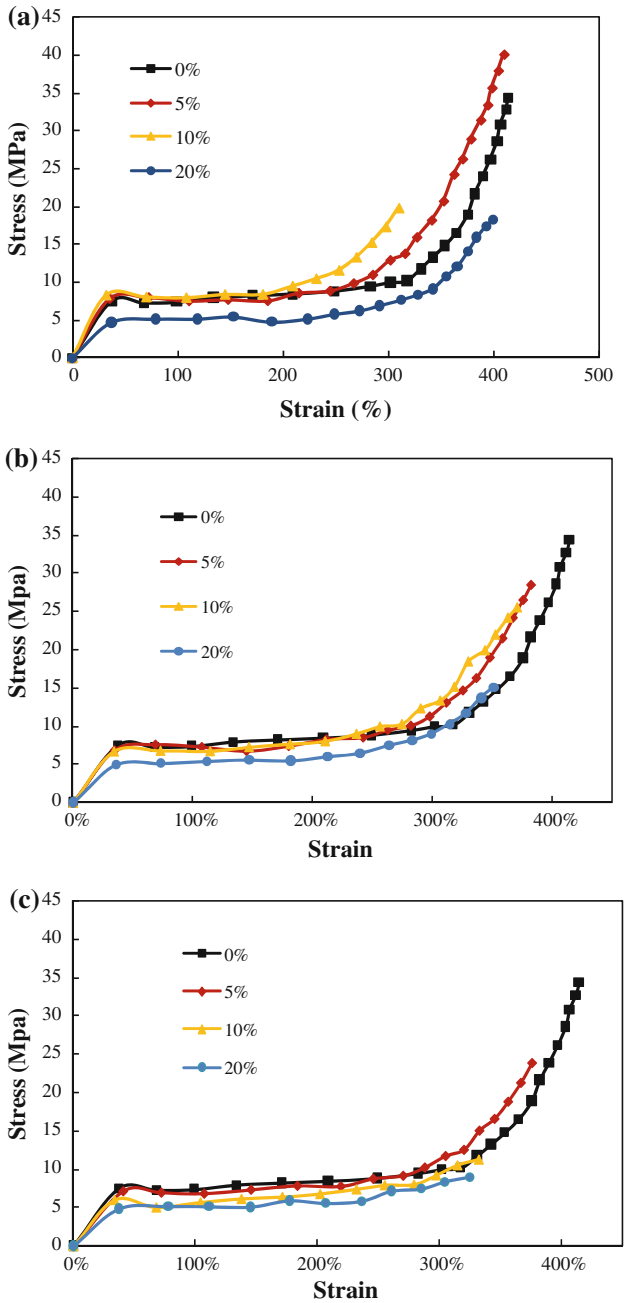

Fig. 3 Representative quasi-static tensile constitutive behavior of FA/PU composites as a function of volume fraction of FA. **a** FA/PU composites filled with small FA particles, **b** FA/PU composites filled with medium FA particles, and **c** FA/PU composites filled with large FA particles

rupture. The first regions of the FA/PU composites and the unfilled PU are almost superposed, which indicates that the Young's modulus, defined as the slope of the engineering stress–strain curve, does not change after introducing FA particles into PU. This is due to the low camera frequency used in our study. When the second picture was taken, the specimen had already yielded. As a result, the modulus of the unfilled PU obtained from the first and the second points of the stress–strain curves shown in Fig. 3 is 23 MPa, lower than Roland's result [25] (27 MPa at a strain rate of 0.06/s). In our later studies, pictures were taken every second for the first 10 s, and the results reveal the Young's modulus of the composites increases with increasing FA content. In the second region of the stress–strain curves, the strain increases from about 35 to 250% while the stress remains nearly constant. In this region, necking starts at a localized point in the specimen, and then increases in length as stretching continues. As a result of this process, molecules are highly orientated. Upon further stretching of the necked specimen, the stress rapidly increases and failure soon occurs [26].

Tensile stress and elongation at break

In Fig. 4, tensile stress at break is plotted versus volume fraction of FA for different FA particle sizes. As can be observed, the unfilled PU studied in this study has a high tensile stress at break (45 MPa). The tensile stress at break decreases with increasing FA content. This is attributed to the debonding of the matrix material from the filler particles. Introduction of rigid particles in a soft matrix always causes localized stress intensification, which may initiate the debonding. The debonded region acts essentially as a void and reduces the tensile stress at break [18]. It can also be seen that the tensile stress at break of the composites increases as the FA particle size decreases. This may result from the fact that larger FA particles are more easily broken.

The simplest model for describing the tensile stress at break of the composites regards the matrix to be the only stress-bearing component:

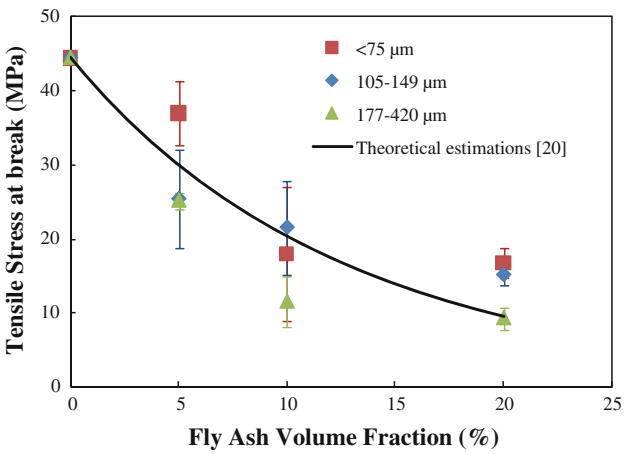

Fig. 4 Tensile stress at break of FA/PU composites as a function of volume fraction of FA (the error bars represent the standard deviation, the central points are the average values of three results)

$$\sigma_c = (1 - \phi)\sigma_m \quad (2)$$

where σ_c and σ_m are the tensile stress at break of the composites and unfilled matrix material, respectively, and $1 - \varphi$ is the effective load bearing cross section of the composites.

An improved description of tensile stress at break is attained by considering the change of the effective cross section as a function of filler volume fraction [27]:

$$\sigma_c = \frac{(1 - V_f)}{1 + 2.5V_f}\sigma'_m \quad (3)$$

where V_f is the volume fraction of FA particles and σ_m' is the tensile stress at break of the matrix of the composites.

The dependence of σ_m' on V_f was best described by the exponential function [27]. The general expression of tensile stress at break is given in the form of:

$$\sigma_c = \frac{(1 - V_f)}{1 + 2.5V_f}\sigma_m \exp(BV_f) \quad (4)$$

where B is a constant. In this study, B is found to be -4.5. A comparison of the tensile stress at break with estimates obtained using the above model is shown in Fig. 4. It can be seen that the theoretical calculations agree well with the experimental results.

The change in elongation at break of the composites, as shown in Fig. 5, corresponds to that in tensile stress at break. The elongation at break also decreases with the addition of FA particles. The special behavior of composites filled with small FA particles, which drops at 10% and then increases at 20% FA loading, is due to the experimental error. For various FA/PU composites, the reduction of elongation at break is not large. When the FA volume fraction is up to 20%, the relative elongation at break is still higher than 0.8.

Moduli at 100 and 300% elongations

The modulus at a particular elongation is given as the tensile stress required to stretch a specimen to that elongation. It is a useful property of an elastomer for engineering applications. Here, based on the stress–strain curves of FA/PU composites, moduli at 100 and 300% elongations are considered.

The dependence of the modulus at 100% elongation with the volume fraction of FA is depicted in Fig. 6. It is seen that the modulus decreases with increasing FA content. The modulus of composites filled with small- or medium-sized FA particles increases a little with a 5% volume fraction of FA and decreases with further addition of FA. There are two major competing phenomena affecting the modulus of the composites. On the one hand, the increase in modulus of the composites is due to the reinforcing ability of the filler. On the other hand, debonding of the matrix from the filler particles occurs during the drawing process. The debonding effect, partly resulting from inadequate matrix material to hold filler particles, is predominant at high volume fractions and leads to the lowering of the modulus. The modulus of composites filled with large FA particles decreases approximately linearly on increasing FA content and is much lower than other composites at low volume fractions of FA. The relative moduli (defined as the modulus of the composites divided by that of the unfilled PU) are 92, 77, and 69% for the composites filled with 5, 10, and 20% large FA particles. This indicates that the large FA particles have no reinforcing ability and the PU matrix becomes the main loading component under such a situation, which may imply the large FA particles have already been crushed when the elongation of the specimen reaches to 100%.

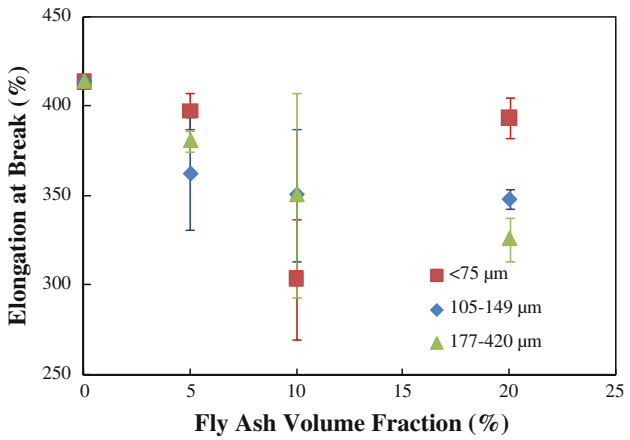

Fig. 5 Elongation at break of FA/PU composites as a function of volume fraction of FA (the error bars represent the standard deviation, the central points are the average values of three results)

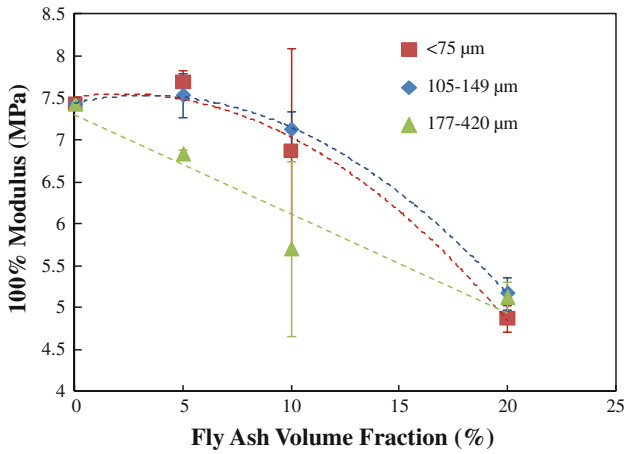

Fig. 6 Modulus at 100% elongation of FA/PU composites as a function of volume fraction of FA (the error bars are standard deviation, the *dashed lines* are trendlines)

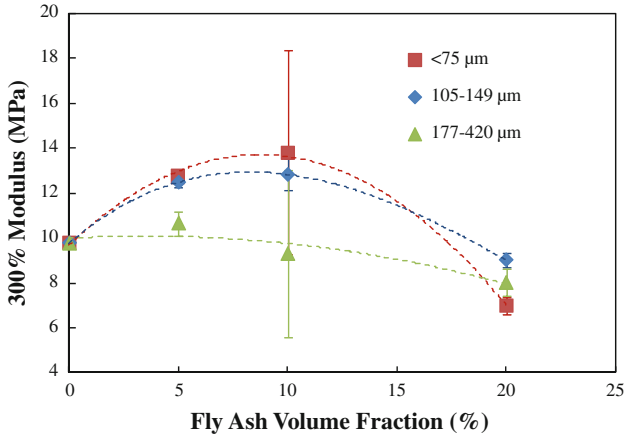

Fig. 7 Modulus at 300% elongation of FA/PU composites as a function of volume fraction of FA (the error bars represent standard deviation, the *dashed lines* are trendlines)

The dependence of the modulus at 300% elongation with the volume fraction of FA is represented in Fig. 7. It can be observed that the modulus of composites filled with small- or medium-sized FA particles increases up to 10% volume fraction of FA and decreases with the further addition of FA. The peak values of both composites are 40% higher than the PU. Alkadasi et al. [19] has reported a similar trend for the 200% modulus of polybutadiene rubber with increasing FA content. As shown in Fig. 2, the specimen has already necked when the elongation of the composites reaches up to 300%. The stress is about to increase dramatically because of the strain hardening. The increase in the modulus at 300% elongation of the composites indicates that the necking process with the composites terminates earlier than with the unfilled PU, due to the pinning and hindering effects of FA particles on the movement of polymer chains. At higher volume fractions, the composites exhibit significant softening. This is also attributed to debonding. Similar to the modulus at 100% elongation, the modulus at 300% elongation of the composites filled with larger FA particles decreases almost linearly as the volume fraction of FA increases.

Fracture surface

Figure 8 shows SEM images of the failure surfaces for the composites with 20% FA particles. It can be seen that the FA particles are homogeneously distributed in the matrix with no signs of agglomerates or holes. It can be clearly observed from these fractographs that most of the FA particles are pulled out from the PU matrix in the composites filled with small- and medium-sized FA particles, while most of FA particles are crushed in the composites filled with larger FA particles. This results in the lower properties of the latter composites.

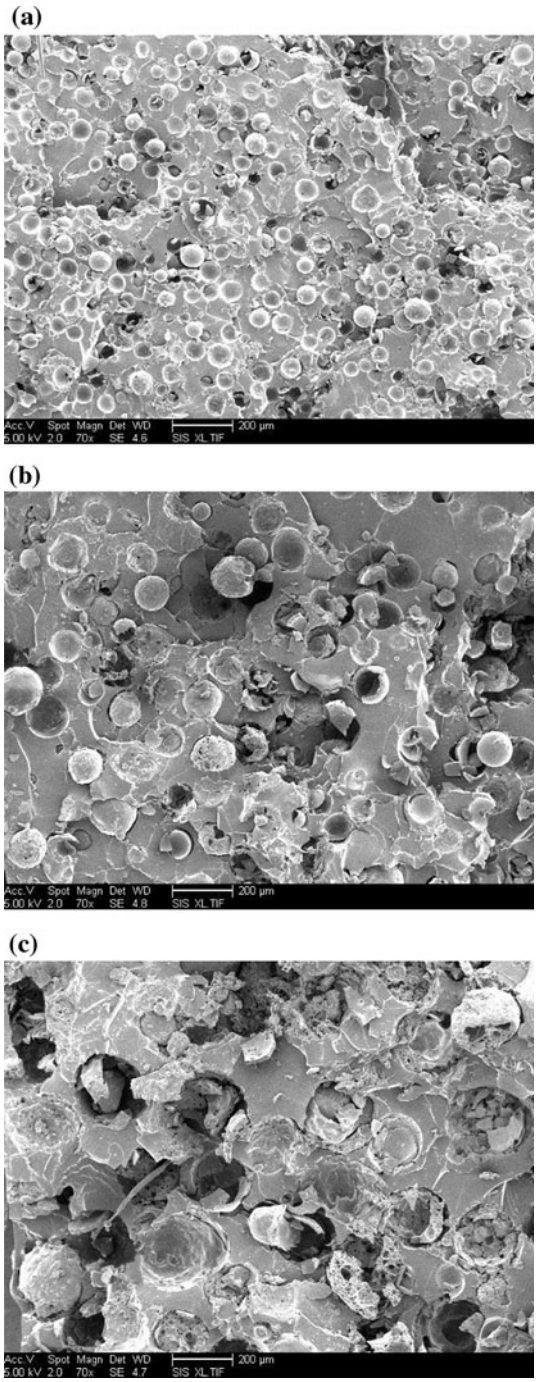

Fig. 8 Fractographs of fracture surface of 20% FA/PU composites with different sizes of FA **a** < 75 μm, **b** 105–149 μm, **c** 177–420 μm

Conclusion

In this article, FA particles with various sizes were introduced into PU, and ten material configurations were prepared. The effects of volume fraction and particle size of FA on the density and tensile properties of these FA/PU composites were studied. The results suggested that the FA

content plays a main role. The density of the composites was observed to decrease linearly with increasing FA content. Adding 20% by volume of FA particles reduces the density by more than 8%. Addition of FA particles decreases the tensile stress and elongation at break of the composites; however, the relative elongation at break of the composites with 20% volume fraction of FA is still higher than 0.8. The moduli at 100 and 300% elongation of the composites filled with small- and medium-sized FA both increase initially, reach a maximum value, and then decrease. The maximum value of the modulus at 300% elongation is 40% higher than that of the unfilled PU. The composites filled with larger FA particles displays inferior properties, compared with the other composites. This may result from the fracture of large FA particles, as can be clearly observed from the SEM images of the failure surface.

Acknowledgement This research has been conducted at the Center of Excellence for Advanced Materials (CEAM) at the University of California, San Diego. The authors would like to acknowledge Prof. Nemat-Nasser and Dr. Amirkhizi for their guidance.

References

1. Li C, Lua J (2009) Mater Lett 63:877
2. Roland CM, Casalini R (2007) Polymer 48:5747
3. Fragiadakis D, Gamache R, Bogoslovov RB, Roland CM (2010) Polymer 51:178
4. Wikipedia (2010) Polyurea. http://en.wikipedia.org/wiki/Polyurea. Last modified on 31 Aug 2010
5. Huntsman Knowledgebase (2001) Tuning the properties of polyurea elastomer systems via raw material selection and processing parameter modulation. http://www.huntsman.com
6. Davini P (2002) Carbon 40:1973
7. Lu GQ, Do DD (1991) Fuel Process Technol 27:95
8. Pandey VC, Abhilash PC, Upadhyay RN, Tewari DD (2009) J Hazard Mater 166:255
9. Fan Y, Yin S, Wen Z, Zhong J (1999) Cem Concr Res 29:467
10. Papadakis VG, Pedersen EJ (1999) J Mater Sci 34:683. doi:10.1023/A:1004500324744
11. Gikunoo E, Omotoso E, Oguocha INA (2005) J Mater Sci 40:487. doi:10.1007/s10853-005-6110-6
12. Wu GH, Huang XL, Dou ZY, Chen S, Jiang LT (2007) J Mater Sci 42:2633. doi:10.1007/s10853-006-1347-2
13. Wu GH, Dou ZY, Jiang LT, Cao JH (2006) Mater Lett 60:2945
14. Dou ZY, Jiang LT, Zhang Q, Xiu ZY, Chen GQ (2007) Scr Mater 57:945
15. Chand N (1988) J Mater Sci Lett 7:36
16. Kishore, Kulkarni SM, Sharathchandra S, Sunil D (2002) Polym Test 21:763
17. Srivastava VK, Shembekar PS (1990) J Mater Sci 25:3513. doi:10.1007/BF00575379
18. Chalivendra VB, Shukla A (2003) J Mater Sci 38:1631. doi:10.1023/A:1023203121299
19. Alkadasi NN, Hundiwale DG, Kapadi UR (2004) J Appl Polym Sci 91:1322
20. Gu J, Wu GH, Zhang Q (2007) Scr Mater 57:529
21. Gu J, Wu GH, Zhang Q (2007) Mater Sci Eng A 452–453:614
22. Nath DCD, Bandyopadhyay S, Yu A, Zeng QH, Das T, Blackburn D, White C (2009) J Mater Sci 44:6078. doi:10.1007/s10853-009-3839-3
23. Rohatgi PK, Matsunaga T, Gupta N (2009) J Mater Sci 44:1485. doi:10.1007/s10853-008-3165-1
24. Qiao J, Amirkhizi A, Schaaf K, Nemat-Nasser S (2011) J Eng Mater Technol 133:011016
25. Roland CM, Twigg JN, Vu Y, Mott PH (2007) Polymer 48:574
26. Nielsen LE (1974) Mechanical properties of polymers and composites. Marcel Dekker, New York
27. Turcsanyi B, Pukanszky B, Tudos F (1988) J Mater Sci Lett 7:160